THE ASTROPHYSICAL JOURNAL, 214:161–178, 1977 May 15

THE OPACITY OF EXPANDING MEDIA: THE EFFECT OF SPECTRAL LINES

ALAN H. KARP, GORDON LASHER, AND K. L. CHAN
IBM Thomas J. Watson Research Center

AND

E. E. SALPETER
Cornell University
Received 1976 July 19; revised 1976 November 8

ABSTRACT

Spectral lines are more effective in slowing the transport of radiation in expanding (or contracting) objects than in static ones. The velocity gradient associated with the expansion causes the frequency of the photons to be continuously redshifted relative to the rest frame of the gas through which they travel. Those photons which are redshifted to the frequency of a sufficiently strong line will be absorbed by the corresponding bound-bound transition, and the net effect will be to increase the effective opacity of the gas. In certain cases the effect can be taken into account by using an effective opacity, the expansion opacity, which is a function not only of the temperature and density but also of the velocity gradient.

Practical formulae for computing the expansion opacity and its Rosseland mean in terms of sums over spectral lines are derived. It is shown that the cumulative effect of many weak lines can be important, implying that a large list of spectral lines is required to obtain results of even modest accuracy. Numerical computations using the 260,000-entry line list of Kurucz and Peytremann have been completed and some samples of the result are given. The general effect may be important in many astronomical objects, but only in some of these will the detailed approach of this paper be appropriate. In optically thick supernova shells, the effect is important both in maintaining the radiation in thermal equilibrium as it diffuses out of the shell and in increasing the value of the total opacity. The enhancement of the opacity ranges from less than 1% to more than an order of magnitude, depending on the temperature, density, and velocity gradient.

Subject headings: opacities — radiative transfer — stars: novae — stars: supernovae — stars: variables

I. INTRODUCTION

The theoretical prediction of the rate of radiation transport in optically thick objects is usually a straightforward application of diffusion theory. The relevant transport coefficient, the Rosseland mean opacity, is obtained by averaging the photon mean free path over the temperature derivative of the Planck function. In static objects the contribution of spectral lines is often small because relatively few photons have frequencies within the narrow spectral lines. In an expanding object, however, the frequency of the photons suffers a continuous Doppler shift with respect to the rest frame of the material, in close analogy to the redshift of photons in the expanding Universe. Thus each photon has an increased probability of interacting with a line. This paper shows that, under certain conditions, this enhanced effect of spectral lines can be taken into account by replacing the ordinary static opacity by an effective opacity, here termed the *expansion opacity*, and applying diffusion theory in the usual manner.

The approach of this paper is largely intuitive. It is based on simple kinetic theory arguments about the mean free path of a typical photon. Contrary to classical diffusion theory, in which one assumes that all conditions change very slightly over a photon mean free path, the expansion opacity applies only if the frequency change of a photon, which is proportional to its mean free path, is large compared with the thermal width of the spectral lines. Although the treatment defines a monochromatic expansion opacity, this concept is not straightforward because each photon has a range of frequencies. The expansion opacity for a given frequency is arbitrarily taken to depend on the mean free path of all those photons which originate at that frequency.

A major aim of this work is to improve the precision of the light curve predictions of models of Type I supernovae computed by Lasher (1975, hereafter Paper I). It was argued in that paper that even weak lines of fairly low-abundance elements will contribute to the effect. The enhanced interaction of the photons with the spectral lines is also necessary in these models to justify the assumption that the radiation remains in thermal equilibrium as it diffuses through the expanding supernova shell.

The fact that the effect of the interaction of radiation and spectral lines is enhanced in moving media has been recognized by others. In particular, Castor (1970, 1974) and Castor, Abbott, and Klein (1975) have considered an effect similar to the one discussed here. Their treatment is quite different from that of this paper because they are considering optically thin objects, namely, stellar atmospheres and winds, where many of the assumptions of this paper are not valid. In spite of this fundamental difference, there are several results that can be applied to both models.

Section II of this paper is a general discussion of radiation transport in an expanding medium. After five days or so from the start of the expansion, the velocity of the gas in a supernova shell is approximately proportional to the radius vector from the center of the shell, and in this case the mean free path of a photon is independent of its direction even when the expansion effects are taken into account. The velocity gradient is uniform throughout the shell and is equal to the reciprocal of the time since the expansion began. In this velocity field one may define an effective opacity which enters the diffusion equation in the usual way. The total opacity, including the enhanced contribution of the spectral lines resulting from the Doppler shift in the expanding shell, will be termed the expansion opacity. The expansion opacity is found to depend on the velocity gradient only through a dimensionless quantity, the *expansion parameter* $s = \kappa_c \rho c t$, where κ_c is the continuous opacity, ρ the density, and t the time since the expansion began. Section II concludes with a discussion of the variation of the expansion opacity with s, showing that it is proportional to s at very small values and falls off as s^{-1} for large values of that of that quantity.

In § III a practical algebraic expression is derived for the expansion opacity in terms of a sum over the spectral lines. A simplified expression for its Rosseland mean is also given. The numerical results for the expansion opacity reported in § IV are given in terms of an enhancement factor ϵ which is simply the fraction of the total expansion opacity due to the spectral lines. The basic information required to calculate the expansion opacity is a list of spectral lines including their frequencies, the excitation energy of their lower levels, and their oscillator strengths. A list of 25,000 lines used by Fowler (1974) for a line-blanketed model of Sirius was found to be inadequate. A longer list with semiempirical oscillator strengths computed by Kurucz and Peytremann (1975) containing 260,000 lines gave a significantly greater expansion opacity. Even this list should be extended to higher frequencies and ionization states in order to be completely adequate for the models of Paper I. The numerical results are given for three abundances, a typical solar abundance, a hydrogen-poor abundance, and a zero hydrogen abundance. These results show that the opacity is increased by a factor of 2 or more over much of the temperature, density, and velocity gradient domain of the models of Paper I. The results thus indicate that the expansion effect is not only sufficient to keep the radiation of the supernova shell Planckian at the local gas temperature as it diffuses through the optically thick shell, but it also significantly increases the total opacity. Section V is a discussion of the assumptions and approximations that are made in the derivations of § III and consequently are reflected in the numerical results of § IV. Section VI concludes the paper with a discussion of possible applications of the expansion opacity to astronomical objects other than supernova shells.

II. RADIATION TRANSPORT IN AN EXPANDING MEDIUM

The fact that spectral lines are more effective in slowing the transport of radiation in expanding objects than in static ones plays an important role in models for supernovae (Paper I). In these models, the presupernova is a supergiant with a degenerate core and an extended envelope consisting of one or two solar masses of material at a density of 10^{-8} or 10^{-9} g cm^{-3}. The core accumulates mass as the envelope material is burned in one or more shells surrounding the core. When the core mass exceeds the stability limit, the core collapses, depositing thermal energy of about 10^{51} ergs at the base of the envelope. A strong radiation-dominated shock wave propagates outward through the envelope and breaks out of the surface; a rarefaction wave then further accelerates the envelope forming a high-velocity shell. After about five days, the hydrodynamic activity ceases, and the material coasts outward at terminal velocity. As the shell becomes optically thin, the radiation diffuses out.

This duffusive release of radiant energy is responsible for the light output of the supernova during the first 30 days, the period of maximum luminosity. The effect of the continuing expansion of the shell and its consequent enhancement of the interaction of the radiation with the spectral lines is important in obtaining correct quantitative results from the model. It is also needed to justify the assumption that the radiation stays Planckian at the local gas temperature as it diffuses out of the shell.

After the shell has moved at a constant velocity for a sufficiently long time, the radius of any portion will be approximately equal to the product of the time t since the beginning of the expansion and the terminal velocity of that portion. Thus the radial velocity v is, simply,

$$\boldsymbol{v} = \boldsymbol{r}/t\,. \tag{1}$$

This velocity field has the property that the relative velocity vector of any two points is simply given by their relative separation divided by the time t.

$$\boldsymbol{v}_{12} = \boldsymbol{v}_1 - \boldsymbol{v}_2 = (\boldsymbol{r}_1 - \boldsymbol{r}_2)/t = \boldsymbol{r}_{12}/t\,.$$

Thus not only the radial-velocity gradient but also the velocity gradient in any arbitrary direction has magnitude t^{-1}. Such a velocity field has an *isotropic velocity gradient*. In the following discussion, it will be seen that the effect of the expansion in decreasing the mean free path of a photon is a function of the velocity gradient. In the presence of an isotropic velocity gradient, the mean free path is independent of the direction of the photon, and the effect is particularly simple. In a general velocity field, the mean free path will be a function of the direction of the photon, and the theory of radiation transport will be more complex.

After 10 days, the density ρ in the supernova shell is very low, about 10^{-12} g cm^{-3}. Examination of a standard opacity table shows that, at such low density, the opacity is due to electron scattering almost exclusively (Cox and Stewart 1970). In the remainder of this paper it will be assumed that electron scattering is the only source of continuous opacity. This assumption simplifies the development, because the electron-scattering opacity is independent of frequency. While there is no difficulty in principle in including any source of continuous opacity, there would be some complications if the frequency variation of the continuous opacity were too rapid.

A photon in the expanding shell suffers a continuous Doppler shift of frequency with respect to the frame of the material at a rate given to order v/c by

$$\frac{d\nu}{dt} = -\left(\frac{\nu}{c}\right)\left(\frac{dv}{dt}\right)_p = -\left(\frac{\nu}{c}\right)\left(\frac{c}{t} - \frac{r}{t^2}\right) \approx -\frac{\nu}{t}\,. \tag{2}$$

The model applies only if the shell is optically thick, and the ratio of the mean free path $\bar{X}$ to the radius r is small. The time of flight of a photon is, in this case, much smaller than the time since the beginning of the expansion,

$$\bar{X}/c \ll r/c = (v/c)t\,.$$

Therefore, the velocity gradient is relatively constant during the flight time of a photon. Equation (2) may be integrated with t constant to give the flight time of the photon t_{01} and thereby the distance x_{01} that it travels while its frequency is shifted from its original value v_0 to its final value v_1,

$$x_{01} = ct_{01} = ct \ln(\nu_0/\nu_1)\,,$$

or

$$\nu_1 = \nu_0 \exp(-x_{01}/ct)\,. \tag{3}$$

This continuous redshift of a photon is like that experienced by a photon in a Friedmann model of the expanding universe.

A helpful understanding of the nature of the expansion opacity is obtained by calculating the effect of a single strong line. The ordinary static opacity has in this case the frequency dependence sketched in Figure 1*a*, where ν_1 is the frequency at line center. Consider a photon whose original frequency ν_0 is slightly greater than the line frequency ν_1. As it travels through the shell, its frequency will continually decrease until it reaches the line (i.e., it has a frequency near ν_1), at which time it will be absorbed in the very strong line. Equation (3) gives the distance the photon must have traveled before being absorbed by the line, namely, $ct \ln(\nu_0/\nu_1)$. By the usual relationship between mean free path and opacity, the expansion opacity at a frequency ν_0 just slightly greater than the line frequency ν_1 is

$$\kappa_{\rm exp}(\nu_0) \approx [\rho ct \ln(\nu_0/\nu_1)]^{-1} = \frac{\sigma_e}{s \ln(\nu_0/\nu_1)}\,, \tag{4}$$

where $s = \sigma_e \rho ct$ is the important dimensionless parameter in determining the expansion opacity. The argument of the expansion opacity $\kappa_{\rm exp}$ was chosen to be ν_0, the initial frequency of the photon. This convention of referring the expansion opacity to the original photon frequency will be kept throughout.

If s is reasonably large, it is equal to the reciprocal of the relative Doppler shift of a photon between electron scatterings. This assertion can be shown by using equation (3) to evaluate the average relative frequency shift from initial frequency ν_0 to final frequency ν, assuming that the photons are subject only to electron scattering,

$$\left\langle\frac{\nu_0 - \nu}{\nu_0}\right\rangle = \langle 1 - \exp(-\bar{X}_\sigma/ct)\rangle \approx \frac{\bar{X}_\sigma}{ct} = \frac{1}{\sigma_e \rho ct} = \frac{1}{s}\,, \tag{5}$$

where $\bar{X}_\sigma = (\sigma_e \rho)^{-1}$ is the scattering mean free path, and the brackets indicate averages over different photon paths. The approximation follows from the assumption that the mean free path is small compared to ct, which is larger than the radius of the shell.

Figure 1*b* is a plot of equation (4) and shows that the single strong spectral line gives rise to a broad structure in the effective opacity. The width of the structure arising from a single strong line is proportional to the reciprocal of the parameter s; that is, if v_0 is close to v_1, the logarithm in equation (4) is approximately equal to

$$\frac{\Delta\nu}{\nu_1} = \frac{\nu_0 - \nu_1}{\nu_1} \approx \frac{1}{s}\left(\frac{\sigma_e}{\kappa_{\rm exp}}\right)\,.$$

If the effective width is defined to be the frequency difference between the points where the line contribution to $\kappa_{\rm exp}$ equals the electron-scattering opacity, then $\Delta\nu_{\rm eff} = \nu_1/s$.

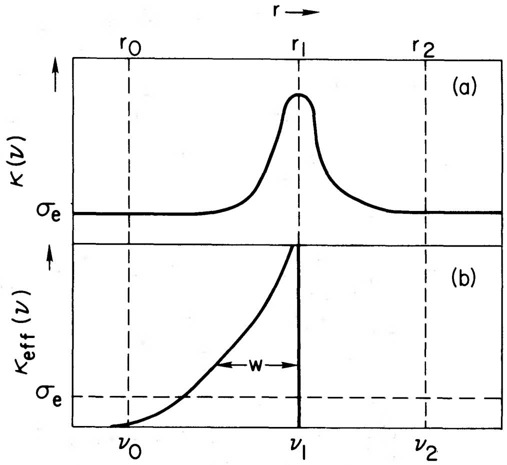

FIG. 1.—(*a*) A sketch of the total static opacity in the vicinity of a spectral line. If the line is not present, on the average a photon starting at a frequency ν_0 will travel a scattering mean free path, $\bar{X}_\sigma = (r_2 - r_0) = (\sigma_e \rho)^{-1}$. If the line is present, the mean free path will be $\bar{X} = (r_1 - r_0) = (\kappa_{eff}\rho)^{-1}$ which is less than $\bar{X}_\sigma$. (*b*) A sketch showing the effective opacity due to an infinitely strong, infinitely narrow line at a frequency ν_1. The width w of the effective profile is inversely proportional to the expansion parameter $s = \sigma_e \rho c t$. The expansion opacity $\kappa_{exp} \approx \kappa_{eff} + \sigma_e$.

Equation (4) is not exact because it neglects the possibility that a photon may be scattered before reaching the line. This simplification was made merely to clarify the argument; the derivation of the general formula for the expansion opacity in the next section will not make this assumption.

Roughly speaking, then, the expansion of the shell broadens the spectral lines to an effective width equal to their frequency divided by the parameter s. It will be shown below that this effective width is the Doppler shift experienced by a photon traveling one scattering mean free path. The effect of strong lines on the Rosseland mean opacity is often small, because the lines are narrow compared with their separation, and only a small fraction of the photons interact with the atomic transitions. If ν/s is greater than the Doppler width, the broadening of the spectral lines by the expansion can, therefore, significantly increase the effective opacity.

When the velocity gradient is sufficiently small, the parameter s^{-1} is much smaller than the typical relative frequency spacing of spectral lines, and the slight broadening of the lines will not affect a large fraction of the photons. In this case, the effect of the expansion on the Rosseland mean opacity will not be important.

On the other hand, at very large values of s^{-1}, a quite different consideration predicts that the increase of the opacity arising from the expansion is small. A large value of s^{-1} implies a large value of the velocity gradient, and the time that a photon stays within the frequency range of a line will be short. In this limit only a small number of atoms will be encountered by the photon while it has the proper range of frequencies, and the probability that it will interact with the atomic transition will be small. In the next section it will be seen that this effect is expressed mathematically by associating an optical thickness with each line that is proportional to s. For small values of s, then, the effect on the Rosseland mean opacity will also be small. When s lies between these extremes, the opacity will be enhanced significantly.

III. DERIVATION OF THE EXPANSION OPACITY

In the preceding section it was shown how the contribution of the spectral lines to the total opacity is enhanced by a velocity gradient and how this enhancement is characterized by the expansion parameter $s = \sigma_e \rho c t$, where t is the inverse of the velocity gradient, the time since the beginning of the expansion. In this section an expression will be derived for the expansion opacity in terms of the strengths and frequencies of the spectral lines by considering the history of a typical photon.

The derivation begins by expressing the mean free path of the photon as the integral of the exponential of the optical depth over distance. The probability that the photon travels a distance x without being scattered or absorbed is $e^{-\tau(x)}$, where $\tau(x)$ is the optical thickness of the material traversed by the photon in traveling a distance x. Given that the photon reaches x, the probability that it is scattered or absorbed in the interval between x and $x + dx$ is $(d\tau/dx)dx$. It follows that the probability that the photon interacts with an element of gas of thickness dx a distance x from its starting point is $e^{-\tau(x)}(d\tau/dx)dx$. The mean free path $\bar{X}$ is the average of x over this weighting function,

$$\bar{X} = \int_0^\infty x e^{-\tau(x)} \frac{d\tau}{dx} dx = \int_0^\infty e^{-\tau(x)} dx, \tag{6}$$

where the second integral is obtained by an integration by parts.

The ith spectral line makes a contribution to the ordinary static opacity equal to $\kappa_i \nu_i \phi(\nu - \nu_i)$ where ν_i is the line center frequency, ϕ is the line profile function normalized to give

$$\int_{-\infty}^{\infty} \phi(\nu - \nu_i) d\nu = 1 ,$$

and κ_i is the line strength with the units of opacity (cm^2 g^{-1}) and having the value,

$$\kappa_i = \frac{\pi e^2}{mc} \frac{f_i}{\nu_i} \frac{N_i}{\rho} \left(1 - \frac{g_i N_u}{g_u N_i}\right) . \tag{7}$$

Here f_i is the oscillator strength of the ith transition; N_i, the number density of the atoms in the lower level of the ith transition. The last factor accounts for the effect of stimulated emission with N_u giving the number density of atoms in the upper level and g_i and g_u the statistical weights of the corresponding levels. In the calculations discussed in § IV, local thermodynamic equilibrium is assumed, in which case the stimulated emission factor becomes $1 - \exp(-h\nu/kT)$.

In the expanding shell, the photon sees not the opacity at a single frequency, but rather the opacity at a frequency which continually decreases with distance x according to the relation given by equation (3). The optical depth of the material traversed by the photon while traveling a distance x must therefore be expressed as an integral over the distance with the integrand evaluated at the proper frequency $\nu(x) = \nu_0 e^{-x/ct}$, where ν_0 is the initial frequency of the photon. This procedure gives,

$$\tau(x) = \int_0^x \left\{ \sigma_e \rho + \sum_{i=1}^{N} \kappa_i \rho \nu_i \phi[\nu(x') - \nu_i] \right\} dx' , \tag{8}$$

where the summation is over all the spectral lines, but in fact only those lines whose frequencies lie in or near the interval from ν_0 to $\nu(x)$ will contribute significantly.

To a good approximation, the line profile function can be replaced by the Dirac (delta) function, thus neglecting the intrinsic line width. This procedure will result in little error in the computed mean free path, if the line width is small compared with the Doppler shift that the photon experiences as it travels a scattering mean free path, a condition which holds in the supernova models. The variable of integration in equation (8) may be changed from distance to frequency by use of equation (3), and with the replacement of the line profile functions ϕ with delta functions, the integration is trivial,

$$\nu_i \int_0^x \delta[\nu(x') - \nu_i] dx' = ct\nu_i \int_{\nu(x)}^{\nu_0} \frac{\delta(\nu' - \nu_i)}{\nu'} d\nu' \begin{array}{l} = ct \text{ if } \nu(x) < \nu_i < \nu_0 , \\ = 0 \text{ otherwise} . \end{array}$$

The result for the optical thickness corresponding to the distance x is

$$\tau(x) = \sigma_e \rho x + \sum_{\nu(x) < \nu_i < \nu_0} \tau_i , \tag{9}$$

where

$$\tau_i = \kappa_i \rho ct = s(\kappa_i / \sigma_e) \tag{10}$$

is now the optical thickness of the ith spectral line. In other words, $\exp(-\tau_i)$ is the probability that the photon will not interact with the ith atomic transition as it is redshifted through the line. This result is just the Sobolev approximation (Sobolev 1957; Castor 1974). The notation below the summation sign indicates that the sum is over only those lines whose frequencies lie between the original frequency of the photon ν_0 and the frequency $\nu(x)$ that it has reached after having traveled a distance x from its origin. Notice that $\tau(x)$ increases linearly with distance until the photon is redshifted into a line; at that point, $\tau(x)$ increases discontinuously by an amount τ_i. In other words, $\tau(x)$ is the sum of a linear function of distance and a series of step functions.

The next step in the derivation is to substitute the expression for the optical depth given in equation (9) into equation (6) for the mean free path $\bar{X}$, and express the resultant integral as a sum of integrals each of which is over a range of x in which the $\tau(x)$ is continuous.

$$\bar{X} = \int_0^{x_J} \exp(-\sigma_e \rho x) dx + \sum_{j=J}^{N} \exp\left(-\sum_{i=J}^{j} \tau_i\right) \int_{x_j}^{x_{j+1}} \exp(-\sigma_e \rho x) dx , \tag{11}$$

where the Jth line is the first one in the line list with a frequency less than ν_0, the lines being in order of decreasing frequency, and x_j is the distance that the photon must travel to be redshifted to the line center frequency ν_j. The integrals are elementary, and the resulting expression can be simplified by rearranging the terms in the sum to give,

$$\frac{\bar{X}}{\bar{X}_\sigma} = 1 - \sum_{j=J}^{N} [1 - \exp(-\tau_j)] \exp\left[-\left(\sigma_e \rho x_j + \sum_{i=J}^{j-1} \tau_i\right)\right] , \tag{12}$$

where $\bar{X}_\sigma = (\sigma_e \rho)^{-1}$ is the electron-scattering mean free path. Equation (3) may be used to express the distances x_j which occur in equation (12) in terms of the line frequencies ν_j. The result yields an expression for the expansion opacity which is the principal algebraic result of this work,

$$\kappa_{\exp}(\nu) = (\rho \bar{X})^{-1} = \sigma_e \left[1 - \sum_{j=J}^{N} [1 - \exp(-\tau_j)](\nu_j/\nu)^s \exp\left(- \sum_{i=J}^{j-1} \tau_i \right) \right]^{-1}, \tag{13}$$

where σ_e is the electron-scattering opacity; $s = \sigma_e \rho c t$ is the expansion parameter introduced in the previous section, ρ being the density, t the inverse of the velocity gradient (i.e., the time since the beginning of the expansion), and ν_j the frequency of the jth line. The sum over j includes all the lines whose frequency is less than ν. The lines are labeled in order of decreasing frequency starting with J for the first line whose frequency is less than the original frequency of the photon and ending with N for the line of lowest frequency. The quantity τ_i is the optical thickness of the ith line given above. The velocity gradient enters the expression for the expansion opacity through the expansion parameters s whose reciprocal is the relative Doppler shift between electron scatterings as well as through the optical thicknesses of the lines, the τ_i, which are proportional to s.

Equation (13) can be written as $\kappa_{\exp}(\nu) = \sigma_e/(1 - \epsilon_\nu)$ where ϵ_ν, the *enhancement factor*, is the fraction of the expansion opacity arising from the mechanism treated in this paper. This quantity is significant because the radiation is thermalized only through the action of the lines and not by the electron scattering. For this reason as well as the fact that it is simply given by the value of the sum in equation (13), the numerical results of the calculation are given in the next section in terms of ϵ_ν and its Rosseland mean.

In the previous section the case was considered for which $\tau_j \gg 1$, implying that the first line encountered by the photon is a very strong one. In this limit, equation (13) reduces to

$$\frac{\bar{X}}{\bar{X}_\sigma} = 1 - (\nu_J/\nu)^s = 1 - \exp(-s x_J/ct) = 1 - \exp(-\sigma_e \rho x_J) . \tag{14}$$

As ν_J approaches ν, the limit of this expression is equal to the intuitive result of the previous section, equation (4), which was obtained by taking the mean free path to be equal to x_J.

Another interesting limit is that of many weak lines whose relative frequency spacing is small compared to s^{-1}, the reciprocal of the expansion parameter. An expression for the expansion opacity can be found for the idealized case of a series of weak lines with the same small optical depth $\tau \ll 1$ and constant frequency spacing Δ. The spacing of weak lines Δ is assumed to be so small that a photon will encounter many lines between electron scatterings, that is, $s\Delta/\nu \ll 1$. From equation (13) the quantity ϵ_ν can be written as

$$\epsilon_\nu = \tau \sum_{j=J}^{N} [1 - (j - J)\Delta/\nu]^s \exp[-(j - J)\tau] ,$$

where the quantity $(1 - e^{-\tau})$ has been approximated by τ. Consecutive terms in the above summation differ by relatively small amounts, and the sum is therefore nearly equal to the integral,

$$\epsilon_\nu \approx \tau \int_0^{\nu/\Delta} (1 - w\Delta/\nu)^s e^{-w\tau} dw .$$

If the expansion parameter s is much greater than unity, the value of this integral can be approximated by replacing the factor $(1 - w\Delta/\nu)^s$ with $e^{-ws\Delta/\nu}$. The upper limit in the resulting integral can be extended to infinity without making any considerable error, and the final result is

$$\epsilon_\nu \approx \left(1 + \frac{s}{\tau}\frac{\Delta}{\nu}\right)^{-1} = \left(1 + \frac{\sigma_e}{\kappa}\frac{\Delta}{\nu}\right)^{-1} , \tag{15}$$

or

$$\kappa_{\exp} \approx \sigma_e \left(1 + \frac{\kappa}{\sigma_e}\frac{\nu}{\Delta}\right) ,$$

where κ is the line strength parameter defined by equation (7). Equation (15) states that the expansion opacity can be considerably greater than the conventional opacity as a result of the cumulative effect of many weak lines if the quantity $(s/\tau)(\Delta/\nu)$ is of the order of unity or less. In any particular case, equation (15) indicates that all lines should be included in calculating the expansion opacity whose optical thickness is of the order of or greater than $s\Delta/\nu$, where Δ is the typical frequency spacing of lines. This quantity can be small compared with unity, and the derived criterion for neglecting weak lines is much more stringent than the obvious one of neglecting those lines whose optical thickness τ is much less than unity. According to equation (15), the expansion opacity in this high density of weak lines limit is independent of the expansion parameter s and therefore of the velocity gradient.

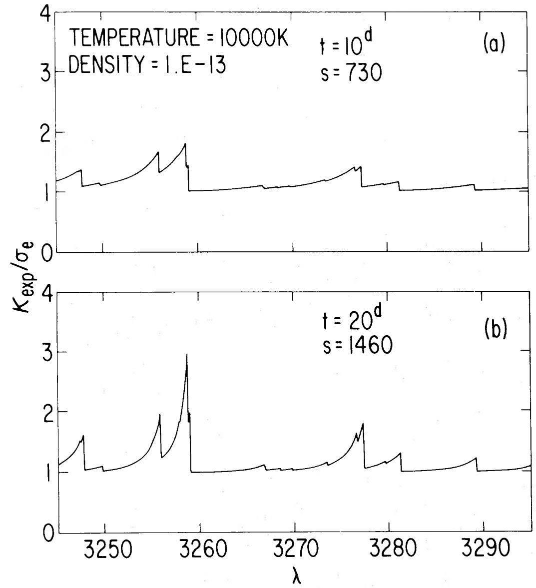

FIG. 2.—The monochromatic expansion opacity in units of the electron scattering opacity for two values of the inverse velocity gradient t. Doubling the expansion parameter doubles the peak opacities but halves the widths of the effective profiles. Only a small subset of all contributing lines was used for this example.

In order to illustrate some of the properties of the expansion opacity that were discussed in § II, the results of a typical calculation of the expansion opacity have been plotted in Figure 2 for two values of the expansion parameter s. As s increases, the peak opacity of each effective line increases while its width decreases. Only a small subset of the contributing lines was used for computing the quantities plotted in Figure 2; a much larger line list was used for the calculations discussed in § IV.

The Rosseland mean opacity is found by averaging the mean free path $\bar{X} = (\kappa_{\exp}\rho)^{-1}$ over frequency, i.e.,

$$\langle \bar{X} \rangle = \frac{\int_0^\infty \bar{X}(\nu)(dB_\nu/dT)d\nu}{\int_0^\infty (dB_\nu/dT)d\nu} = \frac{15}{4\pi^4}\int_0^\infty \bar{X}(u)\frac{dB_u}{dT}du\,,$$

where $u = h\nu/kT$, and B_ν is the Planck function. As in the derivation of the monochromatic expansion opacity, the integral can be broken up into segments that run from one line to the next, giving

$$\langle \bar{X} \rangle = \frac{15}{4\pi^4}\sum_{k=0}^{N}\int_{u_{k+1}}^{u_k} \bar{X}(u)\frac{dB_u}{dT}du\,, \tag{16}$$

where the sum is over some finite list of lines in order of decreasing frequency with two fictitious lines: one at zero frequency, $u_{N+1} = 0$, and one at an indefinitely large frequency, $u_0 = \infty$. These fictitious lines are introduced in order that the summation will include the frequency intervals from $u = \infty$ to the first line and from the last line to $u = 0$. The mean free path $\bar{X}(u)$ in the above equation is, of course, given by $[\rho\kappa_{\exp}(u)]^{-1}$, which may be replaced by the expression in equation (13). The Rosseland mean of the expansion opacity is

$$\langle {\kappa_{\exp}}^{-1}\rangle^{-1} = \frac{\sigma_e}{1 - \langle\epsilon\rangle}\,,$$

where

$$\langle\epsilon\rangle = \frac{15}{4\pi^4}\sum_{k=0}^{N}\sum_{j=k}^{N}[1 - \exp(-\tau_j)]\exp\left(-\sum_{i=k}^{j-1}\tau_i\right)\int_{u_{k+1}}^{u_k}\frac{dB_u}{dT}\left(\frac{u_j}{u}\right)^s du\,. \tag{17}$$

In the limit of s very small, all the τ_j's are very small, and $\langle\epsilon\rangle$ is proportional to s. In the limit of very large s, all the τ_j's become large; the summation over j reduces to a single term, and

$$\langle\epsilon\rangle \approx \frac{15}{4\pi^4}\sum_{k=0}^{N}\int_{u_{k+1}}^{u_k}\frac{dB_u}{dT}\left(\frac{u_k}{u}\right)^s du\,.$$

For closely spaced lines (dB_u/dT) is nearly constant on the intervals u_{k+1} to u_k and can be taken out of the integral, yielding

$$\langle\epsilon\rangle \approx \frac{15}{4\pi^4}\sum_{k=1}^{N}\frac{dB_u}{dT}\bigg|_{u_k} u_k\left\{1-\left(\frac{u_{k+1}}{u_k}\right)^{s-1}\right\}\frac{1}{s-1}\,.$$

Therefore, in both the limits $s \to 0$ and $s \to \infty$, $\langle\epsilon\rangle \to 0$, as expected from the discussion in § II.

IV. NUMERICAL RESULTS

The formalism derived in §§ II and III shows that the opacity can be significantly enhanced by bound-bound transitions if there is a sufficiently large velocity gradient in the gas. Equation (11) shows that the effect depends on the expansion parameter, $s = \sigma_e \rho c t$, which is the reciprocal of the relative Doppler shift between electron scatterings. If the strong lines have a mean relative frequency spacing of less than s^{-1}, a typical photon will encounter a strong line before being scattered, and the expansion opacity will be significantly higher than the normal, static opacity. A line is strong in this context if nearly all photons which are Doppler shifted to the line frequency interact with the line, where the measure of strength is the optical thickness τ defined by equations (7) and (10). In Paper I it was shown that, for typical conditions in a supernova shell ($t = 30^d$, $\rho = 10^{-14}$ g cm^{-3}), $\tau \approx 10^{10} fX$, where f is the oscillator strength of the transition and X is the fractional number abundance of absorbers. In § III equation (15) was derived, showing that a high density of lines with small optical depth can give an expansion opacity significantly larger than the static opacity. For these reasons, lines of rare elements with small oscillator strengths can significantly affect the opacity and must be included in the numerical calculations.

The calculations were based on the abundances shown in Table 1. This list includes all elements occurring in the abundances used by Fowler (1974) that have a normalized number fraction greater than 10^{-10}. It has long been assumed that Type I supernovae are depleted in hydrogen because of the absence of prominent emission lines of Hα

TABLE 1

LOG OF NORMALIZED NUMBER ABUNDANCES*

Normal Hydrogen

X = 0.74 Y = 0.24 Z = 0.02

H −0.036 He −1.106

B	−9.036	Cl	−6.437	Cu	−7.536
C	−3.516	Ar	−5.236	Zm	−7.836
N	−4.076	K	−7.086	Ga	−9.636
O	−3.216	Ca	−5.735	Ge	−9.136
F	−7.437	Sc	−8.815	As	−9.735
Ne	−4.116	Ti	−6.907	Se	−8.836
Na	−5.785	V	−7.636	Br	−9.437
Mg	−4.616	Cr	−6.186	Kr	−8.836
Al	−5.646	Mn	−6.636	Rb	−9.636
Si	−4.516	Fe	−4.437	Sr	−9.186
P	−6.516	Co	−6.936	Zr	−9.536
S	−4.836	Ni	−5.735		

Low Hydrogen

X = 0.10 Y = 0.88 Z = 0.02

H −0.506 He −0.164

All others: renormalize by adding 0.354

Zero Hydrogen

X = 0.0 Y = 0.98 Z = 0.02

H -- He −0.02

All others: renormalize by adding 0.490

*From Fowler (1974); normalized to make sum of abundances unity.

(Minkowski 1939). More recent models of the supernova spectrum computed by Gordon (1975) also require a low hydrogen abundance. Since the immediate objective of these calculations is to provide improved opacity values for models of Type I supernovae, two other abundances were also used, one having a low hydrogen content and the other no hydrogen at all. Therefore, one abundance reflects the effect of processing most of the hydrogen into helium, while in the other all the hydrogen is assumed to have been converted. These abundances are also shown in Table 1. Notice that the mass fraction of the metals is unchanged but that the number abundances must be renormalized. These three abundances will be referred to as normal, low, and zero hydrogen, respectively.

The cumulative effect of many weak lines can be large; it is therefore important to use as large a list of spectral lines as possible. Several test cases were computed using the list of about 26,000 lines included in the calculations of Fowler (1974). The enhancement of the Rosseland mean opacity was found to be typically less than 30%. Examination of the monochromatic expansion opacity showed that there were spectral regions where the line list has very few entries. It was clear that a larger line list was needed. Kurucz and Peytremann (1975) calculated the f-values of all lines from the first five ionization stages of all elements with atomic number up to 30. They then supplemented this list with lines from heavier elements having measured f-values. After removing all lines too weak to make an important contribution, they were left with a set of 260,000 lines. Although any one of the computed f-values may be in error by a large amount, the cumulative effect of all the lines should be reasonably accurate. This line list was used for the calculations described below.

The models of Paper I have a density range of 10^{-8} g cm^{-3} to 10^{-15} g cm^{-3}, a temperature range of 4000 K to 10^5 K, and a velocity gradient corresponding to times of from 2 to 30 days. The original goal of these calculations was to provide expansion opacities for values that bracketed these models but an unexpected difficulty arose. At temperatures above 30,000 K and densities as low as found in the model, most of the abundant elements are ionized at least 5 times. Therefore the line list, as large as it is, is not completely adequate to compute the expansion opacity for the models of Paper I. In addition, there are few lines in the list with a wavelength less than 200 Å that will influence the prediction of X-ray bursts from the shock breakout (Lasher and Chan 1975). The line list is fairly adequate, however, for predicting the optical light curves of supernovae, since the diffusion process is most important in the lower temperature range.

Table 2 shows the value of the expansion parameter s for the entire temperature and density range for which the expansion opacity was computed. In general, the variation in s simply reflects the changes in density. The exception to this rule occurs when an abundant element is changing its degree of ionization, in which case the variation in the number of free electrons per nucleon can be seen by the change in s. The fact that the ionization potential of helium is twice as large as that of hydrogen explains the decrease in s with decreasing hydrogen abundance. This table shows that some of the computed expansion opacities may not be valid, since one or more of the assumed conditions may not hold. In particular, if $s < 1$, then the mean free path of the photon is larger than the envelope, and the assumption that the temperature and density do not vary between emission and absorption of the photon is not valid. In other objects, the velocity gradient may be due to something other than expansion. Even though the gas is still optically thick, s may be small because the velocity gradient is large. In such a situation, these results may be useful but the effect of violating the assumption of an isotropic velocity gradient should be carefully checked (see § V).

The equations of § III and the adopted line list were used to compute the Rosseland mean of the expansion opacity for the three abundances shown in Table 1. These calculations are summarized in Table 3. The results are expressed in terms of the mean enhancement factor, $\langle\epsilon\rangle = 1 - \sigma_e\langle\kappa_{\text{exp}}{}^{-1}\rangle$. Thus, when $\langle\epsilon\rangle$ is small, the effect of the spectral lines is small, and when $\langle\epsilon\rangle$ is near unity, the opacity is dominated by the lines. The opacity enhancement ranges from less than 1% at the highest temperatures to more than an order of magnitude at the lower temperatures in the zero hydrogen case. Even the smallest of the computed enhancements is large enough to thermalize the radiation field as assumed in Paper I. In addition, the calculations show that there is a considerable range of temperatures and densities for which the enhancement is large enough that it must be included in a hydrodynamic calculation.

Several trends can be seen by inspecting Table 3. In general, the opacity enhancement decreases with increasing s. This effect is expected if there are a large number of strong lines. As s increases (i.e., the velocity gradient decreases), the Doppler shift between scatterings decreases and fewer photons will be Doppler shifted to the frequency of a line before being scattered. Only if s is very small, so that the optical depths of most lines, $\tau_i = s(\kappa_i/\sigma_e)$ are small, could this trend be reversed. In this case, there is a good chance that a photon will be Doppler shifted to the frequency of a line, but the probability of interaction with that line will be small. Therefore, increasing s increases the probability of interacting with a line, which, of course, increases $\langle\epsilon\rangle$. However, since the values of κ_i/σ_e are very large compared with unity for many lines, the increase of ϵ with s does not occur unless s is very small.

These trends can be understood by examining Figures 3a and 3b, which show the value of ϵ_ν averaged over 25 Å bands. At 6000 K the peak of the Planck function, B_ν, is near 8000 Å, and the features between 6000 Å and 10000 Å will dominate the Rosseland mean. In the plot for $t = 2^{\text{d}}$, the feature near 6500 Å is due to Hα and the feature near 8500 Å is due to the Ca II infrared triplet. As the velocity gradient decreases, these profiles become narrower and the Rosseland mean of the enhancement factor decreases. Notice that several lines that are weak at $t = 2^{\text{d}}$ are strong at $t = 40^{\text{d}}$. The peak of the band-averaged enhancement factor ϵ decreases when the width of the lines, λ/s, is less than 25 Å. The decrease in ϵ at wavelengths below 200 Å is due to the deficiency in the line list noted

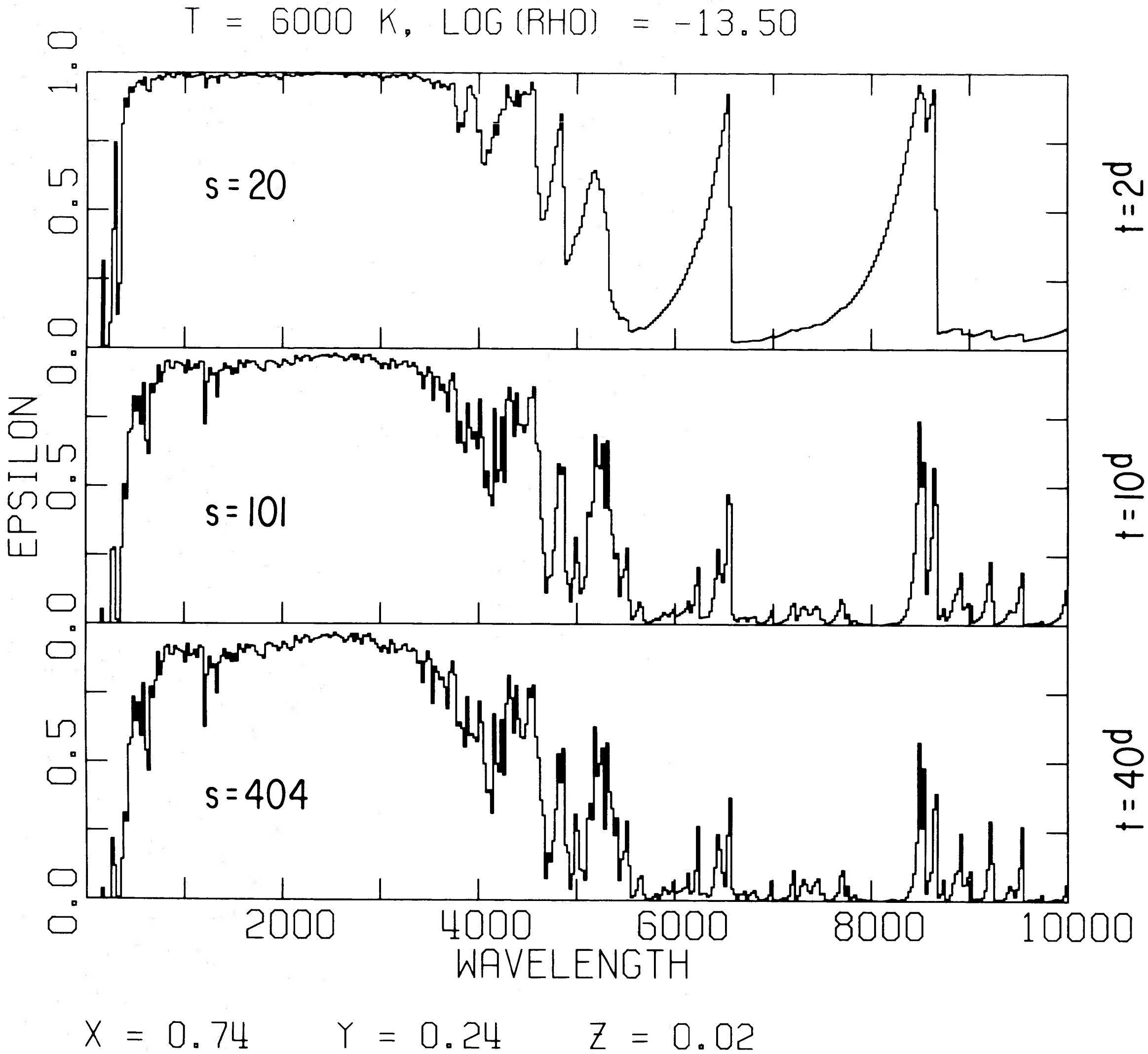

FIG. 3a

FIG. 3.—The opacity enhancement factor ϵ averaged over 25 Å bands for a variety of temperatures and densities. The factor ϵ is the fraction of the total opacity due to the spectral lines enhanced by the mechanism described in the text. When ϵ is near zero, the effect of the lines is small; when ϵ is near unity, the expansion opacity is dominated by line effects. The decrease in ϵ for $\lambda <$ 200 Å is due to a deficiency in the line list. The figures are labeled with both the inverse velocity gradient, t, and the expansion parameter, s. (The solid portions are due to overlapping lines and have no significance.)

above. Figure 3b shows ϵ for $T = 10{,}000$ K and $\log \rho = -13.5$. It is clear that the Rosseland mean opacity is not dominated by only a few lines, as in the previous case, but is due to the cumulative effect of a large number of lines. The narrow dip in ϵ near 1700 Å is a persistent feature of these calculations, and it shows up for a wide range of temperatures and densities. If it is not an artifact of the line list, it should appear as a broad emission feature in the ultraviolet spectrum of a supernova. Of course, extragalactic supernovae are too faint to be observed by satellites, but a similar feature might be seen in novae. The variation of the expansion opacity with increasing s is most dramatic in the case computed for Figure 3c. This case, $T = 26{,}000$ K and $\log \rho = -12.5$, is the highest temperature for which almost all elements are ionized fewer than 5 times, and the line list is adequate. The decrease of ϵ with increasing s is entirely due to the decreasing amount of overlap between effective line profiles. Figure 3d shows ϵ for the same temperature as Figure 3c but for $\log \rho = -12$. Although there is a slight shift in the ionization balance, the principal change is due to the increase of s owing to the increased density.

In general, one would expect the enhancement factor to increase linearly with s at small values of s, attain a more or less smooth maximum, and then decrease as s^{-1}. This is not always the case, however; the actual dependence on s can be more complicated. For example, in the zero hydrogen case in Table 3c, the enhancement factor for $T =$ 6000 K, $\rho = 10^{-14}$ decreases with increasing s between $t = 2^{\rm d}$ and $t = 20^{\rm d}$ and then increases from $t = 20^{\rm d}$ to

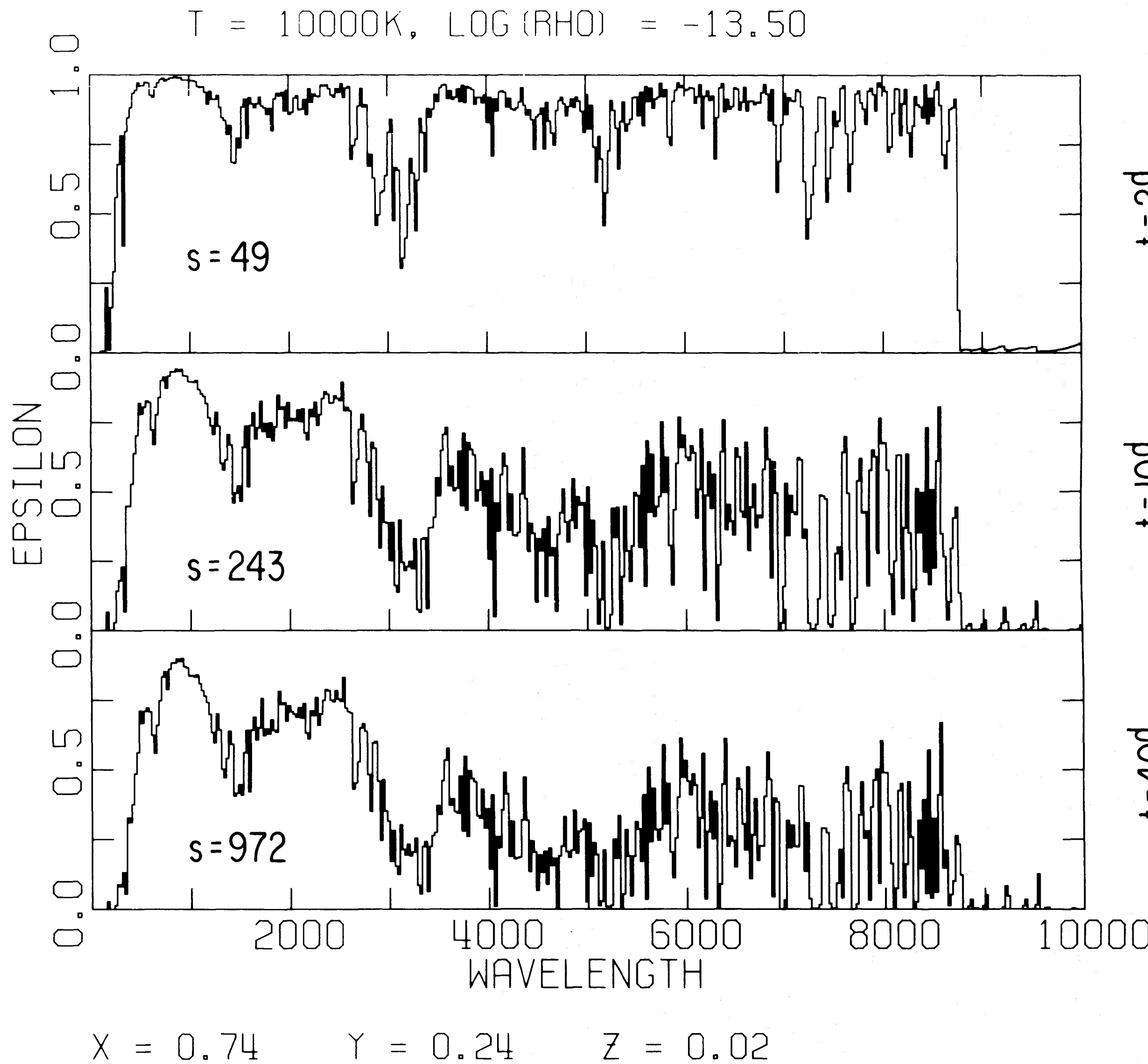

FIG. 3b

FIG. 3.—*Continued*

$t = 50^d$. In this particular case, there is a line with a frequency far from the peak of the Planck function that is so broadened by the velocity gradient that it influences the expansion opacity at small s. As s increases, the effective width of this line decreases until it is no longer broad enough to influence the Rosseland mean enhancement factor, $\langle\epsilon\rangle$. At this point $\langle\epsilon\rangle$ again starts to increase as other lines near the peak of the Planck function become stronger. While this example is rather extreme, there are many places in the tables where the location of the lines relative to the peak of the Planck function is important.

The enhancement of the opacity can be seen quite clearly in Figure 4, which compares the log of the static Rosseland mean opacity with the Rosseland mean expansion opacity. Calculations for two densities are shown; the dashed lines refer to $\rho = 10^{-12}$ g cm^{-3}, the solid lines, to $\rho = 10^{-14}$ g cm^{-3}. In both cases the lower line is the static opacity calculated by Cox and Tabor (1976) using the King IV*a* mixture, which is close in hydrogen abundance to the normal abundance used in this paper. The expansion opacities are for a time t of 10 days. Although the Cox and Tabor opacities include all continuous opacity sources, and the present calculations assume that only electron scattering is important, the expansion opacity is larger than the static value throughout. In particular, notice that the enhancement due to the velocity gradient modifies the electron-scattering opacity more than all other continuous opacity sources combined. This effect can be seen most clearly near log $T = 3.9$, where the Cox and Tabor opacity for *log* $\rho = -12$ rises above the electron-scattering value because of the contribution of other continuous opacity sources. Another significant difference between the static and expansion opacities is the variation with

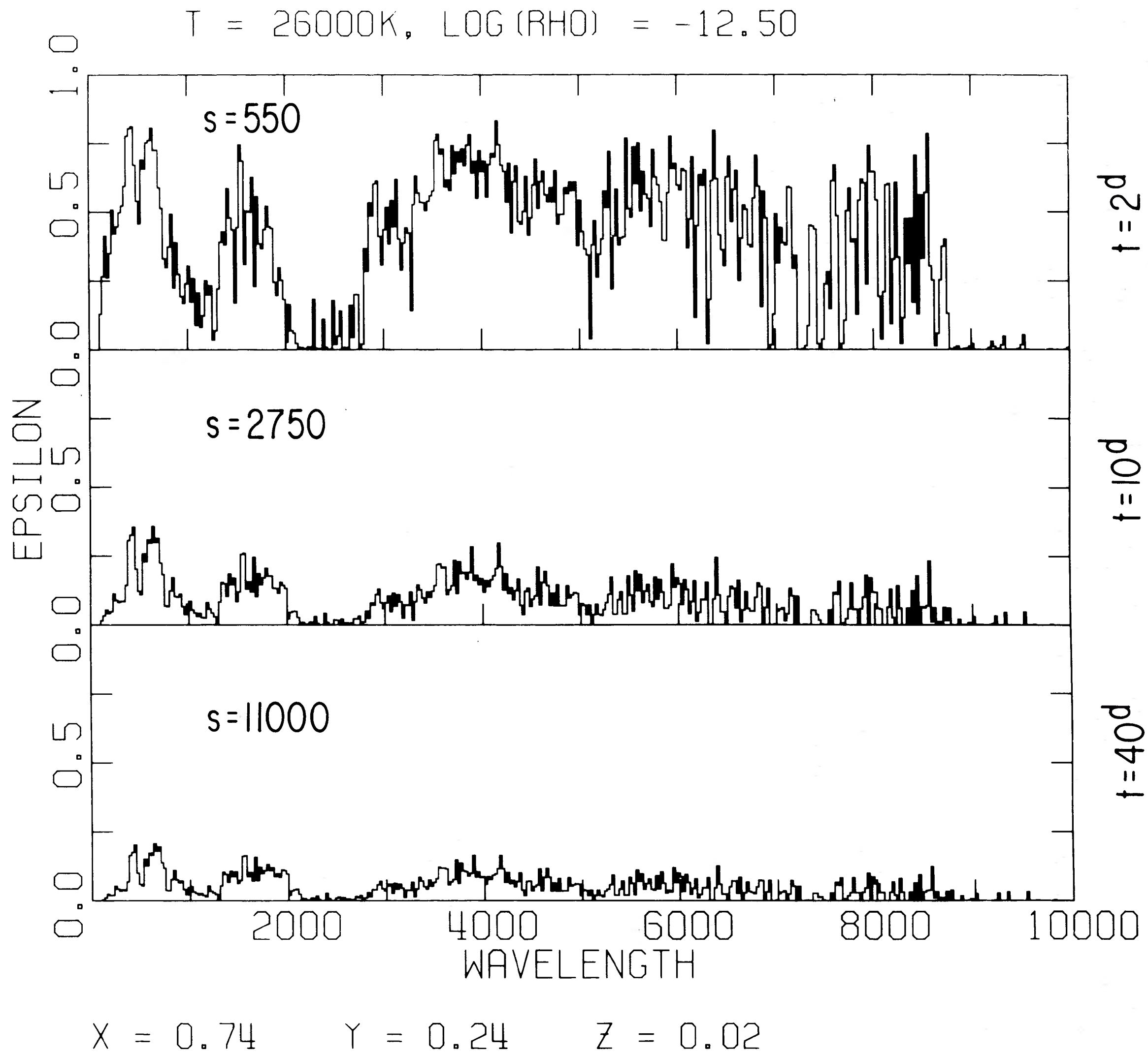

FIG. 3c

FIG. 3.—*Continued*

density. In regions in which the most abundant element is ionized, the static opacity almost always decreases with decreasing density, while, at sufficiently low densities, the expansion opacity increases. This difference may be important for determining the dynamical stability of an expanding gas.

V. ASSUMPTIONS AND APPROXIMATIONS

Several assumptions were made in computing the expansion opacities summarized in § IV. These assumptions fall into three categories: (1) an assumption concerning the physical conditions of the gas which reduces the complexity of the problem—local thermodynamic equilibrium, LTE; (2) assumptions about the various length scales which allow writing the expansion opacity as a function of a single temperature, density, and velocity gradient—isotropic velocity gradient; temperature, and density constant over a photon mean free path; and (3) assumptions concerning the frequency dependence of the static opacity which simplify several integrations—electron scattering as the only continuous opacity source and the Sobolev approximation.

A supernova shell is of low density, so that collisional processes may be relatively ineffective in maintaining the ionization and excitation fractions at their LTE values. However, if the shell is optically thick, the radiation field may still be Planckian. In particular, if the radiation is thermalized over a distance small compared with the

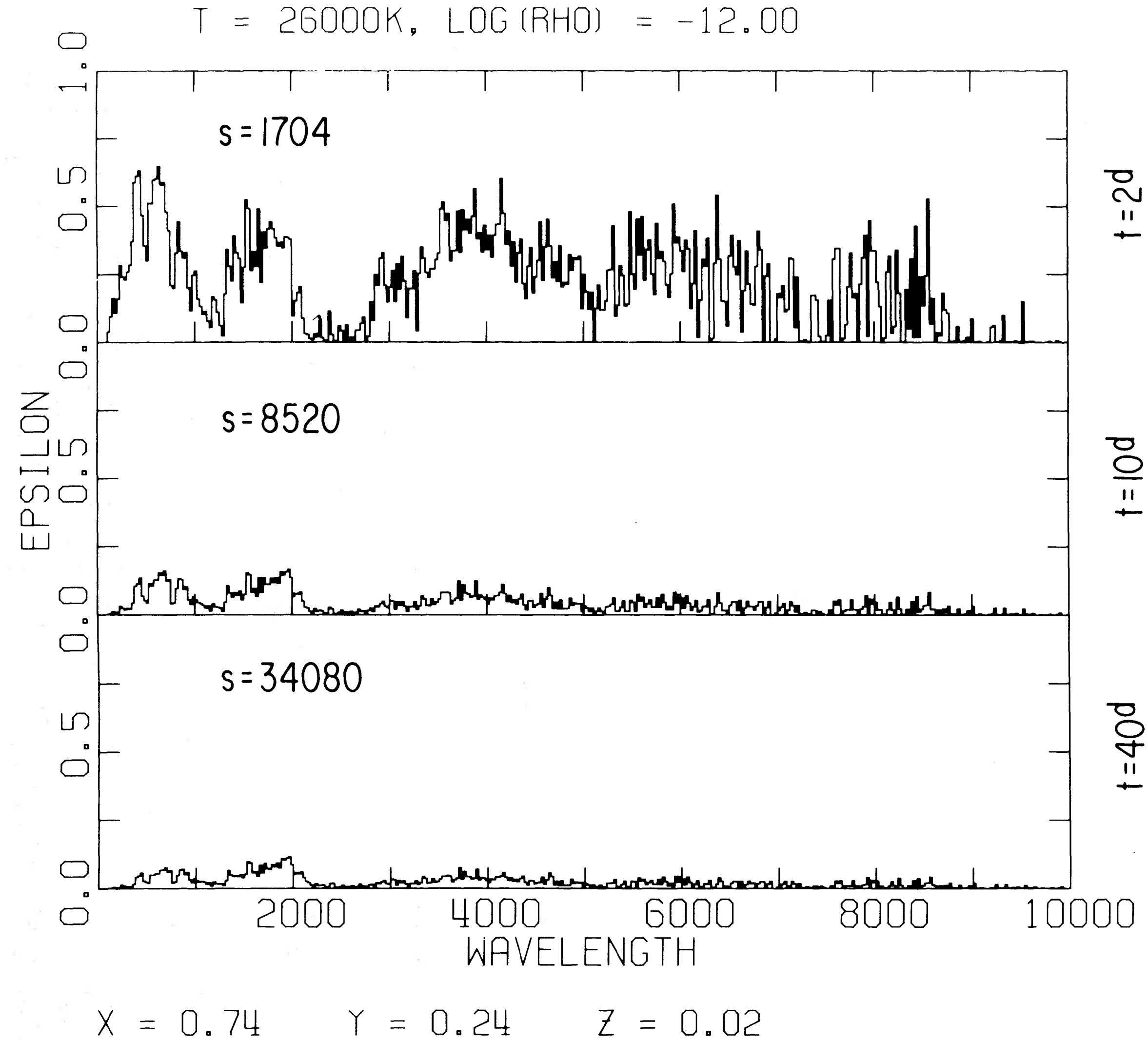

FIG. 3*d*

FIG. 3.—*Continued*

temperature scale height, the radiation will always be Planckian at the local temperature. This condition is equivalent to comparing the relevant scale heights with the thermalization length l_T given by

$$l_T^{-1} = (3\kappa_1 \rho \kappa_{\exp} \rho)^{1/2} = \sigma_e \rho (1 - \langle\epsilon\rangle)^{-1} (3\langle\epsilon\rangle)^{1/2} ,$$

where $\kappa_1 = \langle \kappa_{\exp}{}^{-1} \rangle^{-1} - \sigma_e = \langle\epsilon\rangle \langle \kappa_{\exp}{}^{-1} \rangle^{-1}$ is the part of the opacity by means of which the radiation field is thermalized. Actually, this value of l_T is only a lower limit, since it has been assumed that scattering in the lines is negligible, compared with true absorption, and, therefore, that all the line interactions tend to thermalize the radiation field. The more detailed treatment needed to determine the fraction of the line interactions that result in thermalization of the radiation is beyond the scope of this paper.

If the lines are important, $\langle\epsilon\rangle$ is of order unity and l_T is about a photon mean free path; if the lines make only a small contribution, $\langle\epsilon\rangle$ is small and l_T is large. Examination of Table 3 shows that $\langle\epsilon\rangle$ is typically of the order of $\frac{1}{2}$, which means that l_T is the order of the photon mean free path. Since the models of Paper I are typically more than 50 scattering mean free paths thick, the LTE assumption appears to be reasonable. The fact that the supernova shell is optically thick to electron scattering also implies that the temperature and density do not vary much over a photon mean free path.

In a supernova explosion, the velocity field after a few days is very nearly proportional to the distance from the center of the expansion and has an isotropic velocity gradient (see § II). In most astronomical objects, however, deviations from isotropy will be significant. Castor (1974) has derived an expression for the optical depth of a

TABLE 2*

EXPANSION PARAMETER $s = \sigma_e \rho c t$ FOR t = 1 DAY

Normal Hydrogen

Temperature / Density	6000	8000	10000	14000	18000	22000	26000	30000
1.00(−15)	--	--	--	--	--	--	--	--
3.16(−15)	1.91(+0)	--	--	--	--	--	--	--
1.00(−14)	4.65(+0)	7.61(+0)	--	--	--	--	--	--
3.16(−14)	1.01(+1)	2.40(+1)	2.43(+1)	2.62(+1)	--	--	--	--
1.00(−13)	2.02(+1)	7.55(+1)	7.65(+1)	8.27(+1)	8.28(+1)	--	--	--
3.16(−13)	3.84(+1)	2.34(+2)	2.41(+2)	2.61(+2)	2.62(+2)	2.62(+2)	2.75(+2)	2.82(+2)
1.00(−12)	--	--	7.61(+2)	8.24(+2)	8.28(+2)	8.28(+2)	8.52(+2)	8.90(+2)
3.16(−12)	--	--	--	2.59(+3)	2.62(+3)	2.62(+3)	2.65(+3)	2.79(+3)
1.00(−11)	--	--	--	--	8.27(+3)	8.28(+3)	8.32(+3)	8.70(+3)
3.16(−11)	--	--	--	--	--	--	2.62(+4)	2.69(+4)

Low Hydrogen

Temperature / Density	6000	8000	10000	14000	18000	22000	26000	30000
1.00(−15)	--	--	--	--	--	--	--	--
3.16(−15)	3.20(−1)	--	--	--	--	--	--	--
1.00(−14)	9.35(−1)	1.06(+0)	--	--	--	--	--	--
3.16(−14)	2.49(+0)	3.34(+0)	5.97(+0)	1.06(+1)	--	--	--	--
1.00(−13)	5.85(+0)	1.06(+1)	1.48(+1)	3.36(+1)	3.37(+1)	--	--	--
3.16(−13)	1.24(+1)	3.33(+1)	3.92(+1)	1.06(+2)	1.07(+2)	1.10(+2)	1.62(+2)	1.79(+2)
1.00(−12)	--	--	1.12(+2)	3.32(+2)	3.37(+2)	3.40(+2)	4.57(+2)	5.60(+2)
3.16(−12)	--	--	--	1.03(+3)	1.07(+3)	1.07(+3)	1.27(+3)	1.72(+3)
1.00(−11)	--	--	--	--	3.36(+3)	3.37(+3)	3.65(+3)	5.11(+3)
3.16(−11)	--	--	--	--	--	--	1.10(+4)	1.44(+4)

Zero Hydrogen

Temperature / Density	6000	8000	10000	14000	18000	22000	26000	30000
1.00(−15)	--	--	--	--	--	--	--	--
3.16(−15)	3.01(−3)	--	--	--	--	--	--	--
1.00(−14)	9.39(−3)	7.47(−2)	--	--	--	--	--	--
3.16(−14)	2.91(−2)	1.41(−1)	3.83(+0)	8.16(+0)	--	--	--	--
1.00(−13)	8.94(−2)	2.77(−1)	7.82(+0)	2.58(+1)	2.59(+1)	--	--	--
3.16(−13)	2.68(−1)	5.82(−1)	1.51(+1)	8.12(+1)	8.18(+1)	8.60(+1)	1.45(+2)	1.62(+2)
1.00(−12)	--	--	2.83(+1)	2.55(+2)	2.59(+2)	2.63(+2)	4.01(+2)	5.08(+2)
3.16(−12)	--	--	--	7.84(+2)	8.17(+2)	8.23(+2)	1.07(+3)	1.56(+3)
1.00(−11)	--	--	--	--	2.58(+3)	2.59(+3)	2.96(+3)	4.57(+3)
3.16(−11)	--	--	--	--	--	--	8.62(+3)	1.27(+4)

*Numbers in parentheses are the appropriate power of 10.
The electron density can be found from $\sigma_e = 0.6552 \times 10^{-24}\, N_e/\rho$.

spectral line in a spherically expanding stellar atmosphere that has an arbitrary velocity gradient in terms of a parameter.

$$\Omega = \frac{d(\ln v)}{d(\ln r)} - 1\,,$$

which measures the deviation of the velocity gradient from isotropy. The velocity gradient in any direction is

$$\frac{dv}{ds} = \frac{dv}{dr}(1 + \Omega\mu^2)^{-1}\,,$$

where μ is the cosine of the angle between the radial direction and the direction of the photon. A prime will be used to denote quantities computed with $\Omega \neq 0$. Examination of Table 3 has shown that, over a wide range of temperature and density, the Rosseland mean of the enhancement factor $\langle\epsilon\rangle$ is proportional to s^{-1}. If the velocity gradient is not isotropic, then $s' = s(1 + \Omega\mu^2)^{-1}$, and $\langle\epsilon\rangle' = \langle\epsilon\rangle(1 + \Omega\mu^2)$. Of course, this approximation breaks down if the deviation from isotropy is too large. If the gas is optically thick, the diffusion approximation obtains, and the frequency-integrated specific intensity is approximately

$$I' = B + \mu\frac{dB}{d\tau'} = B + \mu[1 - \langle\epsilon\rangle(1 + \Omega\mu^2)]\frac{dB}{d\tau_\sigma}\,,$$

where $d\tau_\sigma = \sigma_e \rho dx$ is the optical thickness to electron scattering, and $B = (\sigma/\pi)T^4$ is the integrated Planck function. The first moment integral of I' with respect to μ gives the flux

$$H' = \frac{1}{3}\frac{dB}{d\tau_\sigma}[1 - \langle\epsilon\rangle(1 + \tfrac{3}{5}\Omega)]\,.$$

When the velocity gradient is isotropic, the flux is given by

$$H = \frac{1}{3}\frac{dB}{d\tau} = \frac{1}{3}\frac{dB}{d\tau_\sigma}(1 - \langle\epsilon\rangle)\,.$$

It appears that, for those cases in which $\langle\epsilon\rangle \propto s^{-1}$, the effect of a nonisotropic velocity gradient can be approximated by taking $\langle\epsilon\rangle' = \langle\epsilon\rangle(1 + 0.6\ \Omega)$. The result is the same as using the velocity gradient for a single angle, $\mu_{\rm eff} = 0.775$, to represent the mean over all directions.

Another assumption made is that electron scattering is the only source of continuous opacity. Examination of tables of static Rosseland mean opacities and Figure 4 indicates that this assumption is excellent in the Rosseland mean. In certain spectral regions, however, the continuous opacity is considerably larger than the electron-scattering value. Since the enhancement factor is in general proportional to s^{-1}, and s is proportional to the continuous opacity, it is conceivable that ϵ shown in Figures 3 can be an overestimate in several spectral regions. However, the erroneous values of ϵ_ν must be limited to narrow spectral regions or regions far from the peak of the Planck function where the flux is low. If this condition did not hold, the effect would be seen in the static Rosseland mean opacities. Therefore, this assumption has only a small effect on the Rosseland means and a larger, but not excessively large, effect on some of the monochromatic values.

The final assumption made is that the intrinsic line profiles can be approximated by Dirac (delta) functions. This assumption is equivalent to putting all the line opacity at line center, and it has the effect of neglecting the possibility that the photon may be absorbed in the line wings. The error introduced into the mean free path is just the distance between the point in the line wing where the photon is absorbed and line center. The distance is proportional to

TABLE 3

ROSSELAND MEAN OF OPACITY ENHANCEMENT

$<\varepsilon> = 1 - \sigma_e<\kappa_{\rm exp}^{-1}>$

(a) Normal Hydrogen

Temperature / Log density	t(days)	6000	8000	10000	14000	18000	22000	26000	30000
−14.5	2	0.486							
	20	0.393	--	--	--	--	--	--	--
	50	0.356							
−14.0	2	0.527	0.872						
	20	0.389	0.703	--	--	--	--	--	--
	50	0.350	0.573						
−13.5	2	0.506	0.832	0.797	0.760				
	20	0.389	0.572	0.514	0.563	--	--	--	--
	50	0.345	0.443	0.386	0.463				
−13.0	2	0.501	0.748	0.719	0.706	0.623			
	20	0.393	0.452	0.407	0.465	0.371	--	--	--
	50	0.337	0.340	0.296	0.355	0.267			
−12.5	2	0.516	0.635	0.615	0.620	0.589	0.430	0.343	0.287
	20	0.393	0.349	0.316	0.350	0.305	0.182	0.113	0.081
	50	0.328	0.241	0.214	0.235	0.196	0.109	0.060	0.038
−12.0	2			0.510	0.519	0.527	0.363	0.266	0.198
	20	--	--	0.226	0.227	0.213	0.126	0.073	0.040
	50			0.132	0.128	0.116	0.067	0.035	0.017
−11.5	2				0.406	0.426	0.296	0.202	0.126
	20	--	--	--	0.123	0.118	0.074	0.043	0.020
	50				0.059	0.056	0.036	0.020	0.009
−11.0	2					0.289	0.210	0.139	0.081
	20	--	--	--	--	0.054	0.037	0.024	0.012
	50					0.024	0.017	0.011	0.006
−10.5	2							0.081	0.049
	20	--	--	--	--	--	--	0.012	0.008
	50							0.006	0.004

TABLE 3 (cont.)

(b) Low Hydrogen

Temperature / Log density	t(days)	6000	8000	10000	14000	18000	22000	26000	30000
−14.5	2	0.379							
	20	0.503	--	--	--	--	--	--	--
	50	0.474							
−14.0	2	0.588	0.901						
	20	0.506	0.858	--	--	--	--	--	--
	50	0.466	0.807						
−13.5	2	0.621	0.894	0.888	0.829				
	20	0.494	0.806	0.718	0.678	--	--	--	--
	50	0.458	0.716	0.599	0.588				
−13.0	2	0.608	0.878	0.866	0.800	0.713			
	20	0.498	0.713	0.644	0.600	0.479	--	--	--
	50	0.454	0.597	0.520	0.495	0.371			
−12.5	2	0.607	0.837	0.825	0.741	0.683	0.546	0.413	0.345
	20	0.503	0.605	0.561	0.494	0.419	0.274	0.153	0.110
	50	0.445	0.491	0.443	0.377	0.302	0.180	0.085	0.056
−12.0	2			0.756	0.653	0.644	0.475	0.338	0.248
	20	--	--	0.475	0.370	0.334	0.208	0.108	0.058
	50			0.362	0.245	0.210	0.124	0.056	0.026
−11.5	2				0.555	0.566	0.412	0.281	0.166
	20	--	--	--	0.239	0.221	0.140	0.074	0.029
	50				0.132	0.117	0.072	0.036	0.012
−11.0	2					0.445	0.330	0.222	0.112
	20	--	--	--	--	0.116	0.078	0.045	0.017
	50					0.054	0.036	0.021	0.008
−10.5	2							0.150	0.076
	20	--	--	--	--	--	--	0.024	0.017
	50							0.011	0.006

(c) Zero Hydrogen

Temperature / Log density	t(days)	6000	8000	10000	14000	18000	22000	26000	30000
−14.5	2	0.918							
	20	0.553	--	--	--	--	--	--	--
	50	0.435							
−14.0	2	0.806	0.917						
	20	0.539	0.903	--	--	--	--	--	--
	50	0.614	0.897						
−13.5	2	0.687	0.909	0.906	0.848				
	20	0.744	0.902	0.772	0.711	--	--	--	--
	50	0.770	0.893	0.667	0.626				
−13.0	2	0.758	0.908	0.898	0.825	0.742			
	20	0.798	0.900	0.731	0.640	0.516	--	--	--
	50	0.796	0.887	0.616	0.538	0.408			
−12.5	2	0.810	0.910	0.888	0.775	0.712	0.581	0.432	0.361
	20	0.821	0.899	0.693	0.539	0.458	0.307	0.164	0.119
	50	0.795	0.877	0.577	0.424	0.340	0.207	0.093	0.061
−12.0	2			0.874	0.692	0.680	0.513	0.358	0.262
	20	--	--	0.659	0.418	0.376	0.239	0.118	0.063
	50			0.548	0.289	0.247	0.147	0.062	0.028
−11.5	2				0.598	0.608	0.451	0.304	0.177
	20	--	--	--	0.284	0.260	0.167	0.084	0.032
	50				0.165	0.144	0.089	0.041	0.014
−11.0	2					0.494	0.371	0.248	0.120
	20	--	--	--	--	0.144	0.097	0.054	0.019
	50					0.068	0.046	0.025	0.009
−10.5	2							0.177	0.084
	20	--	--	--	--	--	--	0.030	0.013
	50							0.014	0.006

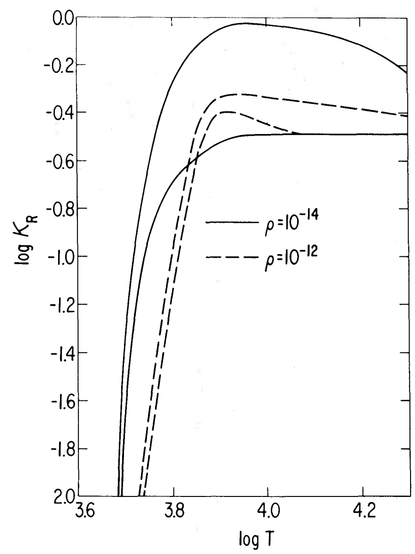

FIG. 4.—The log of the Rosseland mean opacity versus the log of the temperature for densities of $\rho = 10^{-12}$ g cm^{-3} (*dashed line*) and $\rho = 10^{-14}$ g cm^{-3} (*solid lines*). All cases were computed with an abundance of $X = 0.74$, $Y = 0.28$, $Z = 0.02$. In each case the lower curve is the static opacity of Cox and Tabor (1976), and the upper curve is the expansion opacity computed using the method described in the text with *a* time $t = 10^d$.

the Doppler width. Since the thermal velocity of a metal atom is typically less than 3 km s^{-1} for the cases computed above, the relative Doppler width is $\Delta\nu/\nu \approx 10^{-5}$. An error of a factor of 2 in the mean free path could be made if this is equal to the relative Doppler shift between electron scatterings, s^{-1}. Examination of Table 3 shows that $\langle\epsilon\rangle$ is always small when $s^{-1} < 10^{-4}$. Therefore, the relative error in the enhancement factor due to this assumption is large only when the opacity enhancement is negligibly small.

VI. SUMMARY AND CONCLUSIONS

A supernova explosion is one of the most violent events in the Universe. There is an understandable tendency, therefore, to consider phenomena associated with supernovae as extremes inapplicable to other objects. Such is not the case for the velocity gradients considered in this paper. To put things in perspective, a velocity difference of 1 km s^{-1} over a distance of a solar radius corresponds to an inverse velocity gradient t of 10 days, a value characteristic of the supernovae models of Paper I. This result indicates that there may be many astronomical objects in which the expansion opacity is significantly larger than the static opacity. Table 4 summarizes some possible applications of these calculations other than supernovae. The table entries in most cases were read from a figure appearing in the literature. They are not precise, but they serve to indicate whether or not the phenomenon discussed in this paper applies. In most cases the value of the continuous opacity used to compute the expansion parameter s was taken from Alexander (1975). As a general rule of thumb, if the expansion parameter s is of the order of 10^4 or greater, the enhancement factor $\langle\epsilon\rangle$ will be small. On the other hand, if s is of the order of 10^3 or

TABLE 4

EXPANSION PARAMETER $s = \kappa_c \rho c t$
FOR INTRINSIC VARIABLES

Type of Object	Δv(km s^{-1})	t(days)	log ρ	κ_c	s	reference
nova	2000	1	−11	0.003	<100	Starrfield, *et al.* (1974)
Mira variable	2	40	−12	0.01	1000	Maciel (1976)
Long period variable	2	120	−10	0.001	30000	Hill (1976)
Cepheid	5	1	−9	0.005	<2000	Karp (1975)
RR Lyrae	5	0.1	−8	0.1	500000	Hill (1972)
protostar	20	600	−15	0.15	$\lesssim$1000	Larson (1972)
Of star	100	0.5	−12	0.3	<1000	Castor, *et al.* (1975)

less, the contribution of the lines to the total opacity will be significant. Only in the photospheres of the long-period variables and RR Lyrae stars is the enhancement negligibly small. In the novae, on the other hand, the lines probably dominate the opacity. The results of this paper cannot be applied directly to most of these objects, since, in general, the density scale height is comparable with the photon mean free path. The table does indicate, however, that the enhancement of the opacity by the Doppler effect should be considered.

To summarize, this paper has made the following points:

1. The probability that a photon will be absorbed in a spectral line is greatly enhanced in the presence of a velocity gradient. It was shown that this effect decreases the mean free path of a typical photon and, therefore, increases the effective opacity of the gas. In the case of optically thick supernova shells, it is useful to define a monochromatic expansion opacity which is inversely proportional to the mean free path of the photon. This expansion opacity depends on the velocity gradient through the expansion parameter $s = \kappa_c \rho c t$, where κ_c is the continuous opacity, ρ the mass density, and t the inverse of the velocity gradient.

2. While the strong lines are obviously important, it was shown that a high density of weak lines can also make a large contribution to the expansion opacity. An expression was derived for the monochromatic expansion opacity in terms of the strengths and frequencies of the spectral lines and the expansion parameter, s. This expression was then integrated to give the Rosseland mean expansion opacity, $\langle \kappa_{\mathrm{exp}}{}^{-1} \rangle^{-1}$. In both cases the derived expressions are general in that they allow for the effects of the continuous opacity and overlap of the effective line profiles.

3. A line list of 260,000 atomic transitions compiled by Kurucz and Peytremann (1975) was used to evaluate the expansion opacity for a wide range of temperatures, densities, and velocity gradients, including those values expected in a supernova envelope. It was found that the line list was adequate only for temperatures less than 30,000 K and wavelengths greater than 200 Å. The range of opacity enhancements was found to be large. At the highest temperatures and densities, the relative enhancement was small, changing the static opacity by less than 1%. Although this effect need not be used to modify the opacities, it may be important for keeping the radiation in thermal equilibrium, thereby justifying the use of the diffusion approximation in Paper I. On the other hand, at the lower temperatures and densities, the expansion opacity ranges from a factor of 2 to more than an order of magnitude larger than the static opacity, and therefore will change the quantitative results of hydrodynamic models like those of Paper I. In this case, the enhancement effects must be included in any hydrodynamic calculation.

4. The velocity gradients in supernovae are of the same order of magnitude as those found in several other astronomical objects. The opacity enhancement may well be significant in several such cases.

We would like to thank J. Niebuhr and Dr. D. Fischel for supplying data tapes containing the line lists and Dr. C. Gordon for many helpful discussions.

REFERENCES

Alexander, D. R. 1975, *Ap. J. Suppl.*, **29**, 363.
Castor, J. I. 1970, *M.N.R.A.S.*, **149**, 111.
———. 1974, *M.N.R.A.S.*, **169**, 279.
Castor, J. I., Abbott, D. C., and Klein, R. I. 1975, *Ap. J.*, **195**, 157.
Cox, A. N., and Stewart, J. N. 1970, *Ap. J. Suppl.*, **19**, 243.
Cox, A. N., and Tabor, J. E. 1976, *Ap. J. Suppl.*, **31**, 271.
Fowler, J. W. 1974, *Ap. J.*, **188**, 295.
Gordon, C. 1975, *Ap. J.*, **198**, 765.
Hill, S. J. 1972, *Ap. J.*, **178**, 793.
———. 1976, *Bull. AAS*, **8**, 428.
Karp, A. H. 1975, *Ap. J.*, **199**, 448.
Kurucz, R. L., and Peytremann, E. 1975, "Smithsonian Ap. Obs. Spec. Rept.," No. 362.
Larson, R. B. 1972, *M.N.R.A.S.*, **157**, 121.
Lasher, G. 1975, *Ap. J.*, **201**, 195 (Paper I).
Lasher, G., and Chan, K. L. 1975, *Bull. AAS*, **1**, 505.
Maciel, W. J. 1976, *Astron. Ap.*, **48**, 27.
Minkowski, R. 1939, *Ap. J.*, **89**, 156.
Starrfield, S., Sparks, W. M., and Truran, J. W. 1974, *Ap. J. Suppl.*, **28**, 247.
Sobolev, V. V. 1957, *Soviet Astr.–AJ*, **1**, 297.

K. L. Chan: Physics Department, University of Calgary, Calgary, Alberta T2N1N4, Canada

Alan H. Karp: Department of Physics and Astronomy, Dartmouth College, Hanover, NH 03755

Gordon Lasher: IBM Thomas J. Watson Research Center, P. O. Box 218, Yorktown Heights, NY 10598

E. E. Salpeter: 308 Newman LNS, Cornell University, Ithaca, NY 14853